Angewandte Chemie
Eine Zeitschrift der Gesellschaft Deutscher Chemiker

Supporting Information

© Wiley-VCH 2005

69451 Weinheim, Germany

An Unprecedented Germanate Framework Containing 24-Ring Channels, Ni-Ge Metal Bonds, and Chiral [Ni@$Ge_{14}O_{24}(OH)_3$] Cluster Motifs Transferred from Chiral Metal Complexes**

Zhi-En Lin**, **Jie Zhang**, **Jing-Tai Zhao**, **Shou-Tian Zheng**, **Chun-Yang Pan**, **Guo-Ming Wang**, and **Guo-Yu Yang*

Supporting Materials:

Supporting Figures:

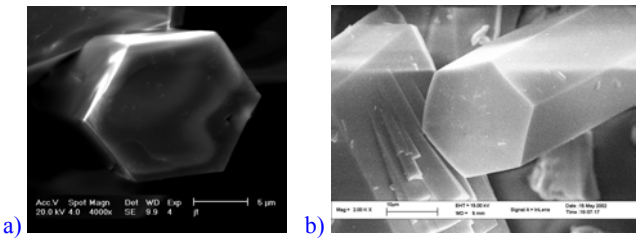

Figure S1. SEM images showing the morphology of as-synthesized crystals of FJ-1a and FJ-1b: a) $Ni@Ge_{14}O_{24}(OH)_3{\cdot}2Ni(en)_3$, FJ-1a; b) $Ni@Ge_{14}O_{24}(OH)_3{\cdot}2Ni(enMe)_3$, FJ-1b.

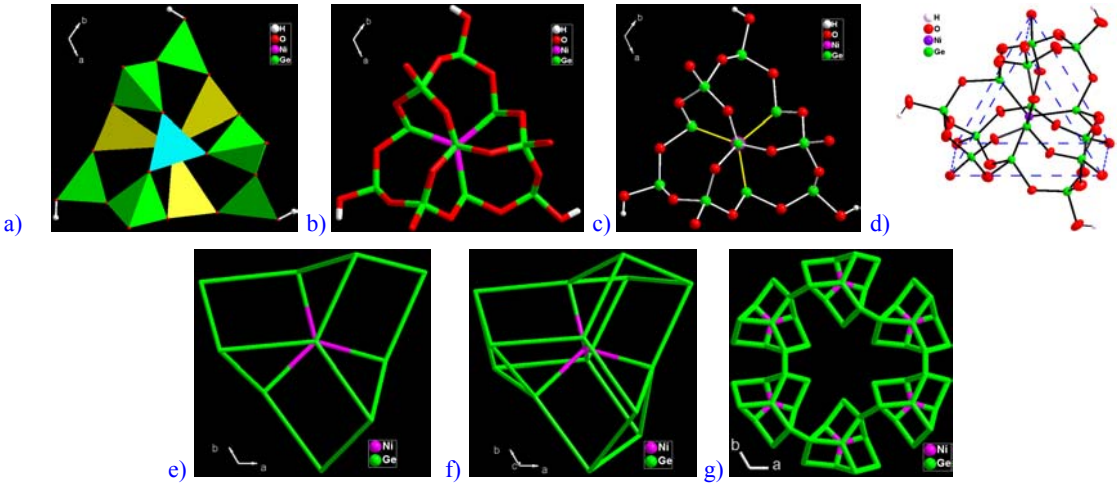

Figure S2. a) The polyhedral representation of the inorganic structural motif of $[Ni@Ge_{14}O_{24}(OH)_3]^{4-}$ ($Ni@Ge_{14}$) cluster as building unit along the *c* axis. Color code: green $Ge(1,2)O_4$ tetrahedra; cyan $Ge(3)O_3Ni$ tetrahedra; yellow $Ge(4)O_3Ni$ tetrahedra, respectively. b) The topological structure of $Ni@Ge_{14}$ cluster containing Ge, Ni, O and H atoms along the *c* axis. c) The ball-stick representation of $Ni@Ge_{14}$ cluster along the *c* axis. d) The $Ni@Ge_{14}$ cluster can be seen as a trigonal-prismatic building unit in FJ-1a framework along approximate the *c* axis. This building unit is connected to six others exclusively through vertex oxygen atoms to form 3D framework. e-f) The topological structure of $Ni@Ge_{14}$ cluster containing only Ge and Ni atoms. g) The topological structure of the single 24-ring channel linked six $Ni@Ge_{14}$ motifs along the *c* axis, showing the Ge-Ge and Ge-Ni linkages.

As shown in Figure S2, the Ni1 atom locates in the center of the $Ni@Ge_{14}$ cluster motif with C_3 symmetry. There exists a rare trigonal bipyramidal {$Ni@Ge_5$} core with D_{3h} symmetry in the $Ni@Ge_{14}$ motif.

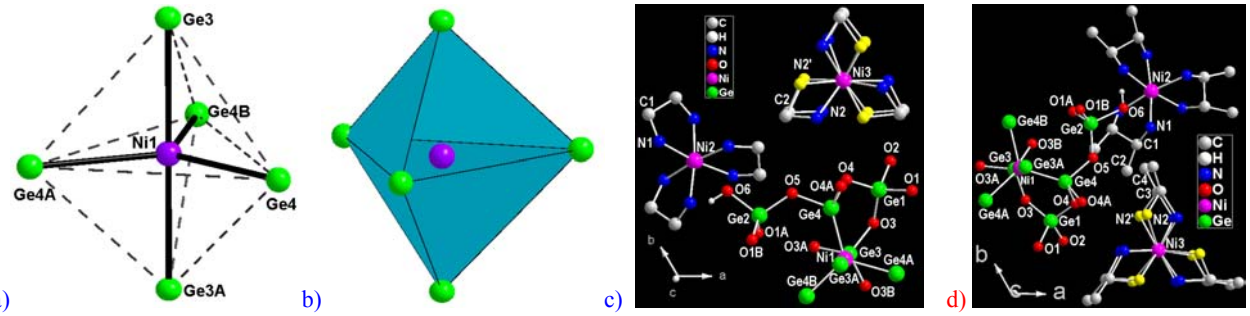

Figure S3. a) Ball-and-stick and b) polyhedral representations of the $Ni@Ge_5$ core with trigonal bipyramid coordination geometry (color code: Ni purple, Ge green). c) View of the coordination environments of Ni and Ge atoms in the asymmetric unit in FJ-1a and FJ-1b, showing N2 blue, N2' yellow. The C2 and C4 (methyl of the enMe) atoms in FJ-1b are disorder and have occupancies of 0.5.

As shown Figure S3a-d, the Ni1 atom as μ_5-bridge locates in the center of the {$Ni@Ge_5$} core with a trigonal bipyramidal geometry. The Ni^{+}-Ge^{2+} distances vary in the range 2.251(2)-2.317(2) Å (Ni1-Ge3, 2.251(2) Å; Ni1-Ge4, 2.317(2) Å), which are close to the distances of Ni^0-Ge^{2+} bonds of GeO_3Ni tetrahedron in the compound, $[(CO)_3Ni^0\text{-}Ge^{II}(OtBu)_2]_2$ (Ni^0-Ge^{2+} bond, 2.283(2) Å) (see to reference 10a in text) and other Ni^0-Ge^{2+} bonds (2.206-2.291Å) in nickel-germylene complexes (see to reference 10b-d in text), but the Ni^{+}-Ge^{2+} distances are considerably shorter than the Ni-Ge bond (2.338(2)-2.487(2) Å) in zintl anions of $[K(2,2,2\text{-crypt})]_4[Ni\text{-}Ni\text{-}Ni@(Ge_9)_2]$ (see to J. M. Goicoechea, S. C. Sevov, *Angew. Chem.* **2005,** *117*, 4094; *Angew. Chem. Int. Ed.* **2005**, *44*, 4026).

In Figure S3c/d, the Ge1/Ge2 atoms make four Ge-O bonds to form GeO_4 tetrahedra (In FJ-1a, Ge-O 1.722(10)-1.766(7) Å, O-Ge-O 99.3(4)-115.3(6)º; in FJ-1b, Ge-O 1.688(15)-1.769(16) Å, O-Ge-O 99.8(6)-115.0(5)º). These values are in agreement with those of the 4-connected germanate framework); the Ge3/Ge4 atoms make only three Ge-O bonds and one Ge-Ni bond to form GeO_3Ni tetrahedra (In FJ-1a, Ge-O 1.803(9)-1.849(7) Å, Ge-Ni 2.251(2)-2.317(2) Å, O-Ge-O 94.1(3)-98.1 (3)º and O-Ge-Ni 119.9(2)-124.9(3)º; in FJ-1b, Ge-O 1.808(15)-1.827(12) Å, Ge-Ni 2.252(2)-2.317(2) Å, O-Ge-O 95.6(9)-98.3 (4)º and O-Ge-Ni 120.6(4)-122.4(5)º). Thus the Ge1/Ge2 are typical Ge^{4+} atom in FJ-1a and FJ-1b. The Ni1 atom bonds five Ge (three Ge4 and two Ge3) atoms to yield a trigonal bipyramid, {Ni@Ge_5} core (Ni-Ge, 2.251(2)-2.317(2) Å), indicating Ni1, Ge3/Ge4 atoms in FJ-1a and FJ-1b are low-valent atoms. Interestingly, there are two types of $[Ni(en)_3]^{2+}$/$[Ni(enMe)_3]^{2+}$ complexes in FJ-1a/FJ-1b (Figure S3c/d). One is a regular octahedral chiral $[Ni2(en)_3]^{2+}$/$[Ni(enMe)_3]^{2+}$ complex with D_3 symmetry (Ni2-N1 2.049(14)/2.03(4) Å for FJ-1a/FJ-1b), another is a rare trigonal prismatic achiral $[Ni3(en)_3]^{2+}$/$[Ni(enMe)_3]^{2+}$ complex with D_{3h} symmetry (Ni3-N2/Ni3-N2', 2.265(18)/2.047(19) Å and 1.97(4)/2.38(3) Å for FJ-1a and FJ-1b, respectively). Owing to the requirement of the structural symmetry, the unique N atoms coordinated to Ni3 center occupy two split positions of N2 and N2' (N2···N2', 1.65(2)/1.71(4) Å in FJ-1a/FJ-1b) and have occupancy of 0.5. Six N2 and six N2' atoms bond Ni3 atom to form two sets of rare trigonal prismatic geometries, respectively. Assuming the valence of Ge(1,2), Ge(3,4), Ni1, Ni(2,3), O and H to be +4, +2, +1, +2, –2 and +1, respectively, the framework stoichiomentry of $[Ni@Ge_{14}O_{24}(OH)_3]^{4-}$ creates a net framework charge of -4 which can be balanced by two $[Ni(en)_3]^{2+}$ (one is $[Ni2](en)_3)^{2+}$, another is $[Ni3](en)_3]^{2+}$) complex cations, indicating that there exists in deed low-valent Ni^{+} and Ge^{2+} ions in the Ni@Ge_{14} unit confirmed by magnetic and luminescent measurements.

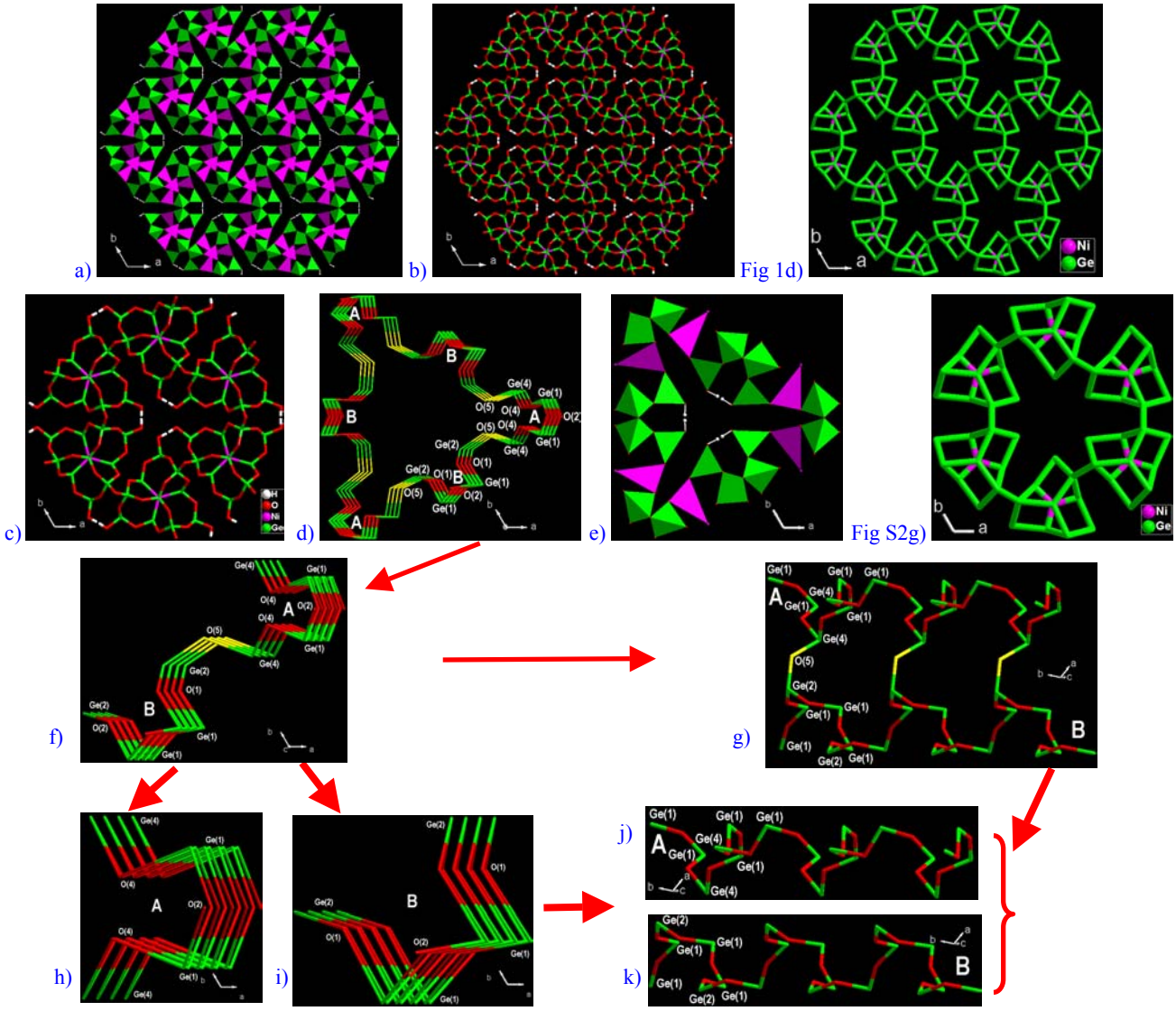

Figure S4. a) and b) The polyhedral and topological representation of the open-framework of FJ-1a. c) The topological structure of the single 24-ring channel constructed from six Ni@Ge_{14} clusters. d) The topological structure of the single 24-ring channel constructed from six puckered chains with both three A type and three B type linked alternate by shared O(5) atoms through Ge4-O5-Ge2 linkages. e) The polyhedral representation of the single 24-ring channel delimited by eighteen GeO_4 (green, Ge(1,2)O_4 tetrahedra) and six GeO_3Ni tetra-

hedral (purple, $Ge(4)O_3Ni$ tetrahedra). f) View of adjacent A- and B-type chains linked O(5) atoms. g) View of the extended adjacent A- and B-type chains. h) and i) View of adjacent two puckered chains with A- and B-type, respectively. j) and k) View of the extended A- and B-type chains.

There are six puckered chains with the A- and B-type linked alternately through sharing O5 atoms via Ge4-O5-Ge2 linkages in the 24-ring channel (Figure 4d). Adjacent A- and B-type chains are made of the unclosed -Ge1-O2-Ge1-O4-Ge4-O4 -Ge1-O2-Ge1-O4-Ge4-O4- and -Ge1-O2-Ge1-O1-Ge2-O1-Ge1-O2-Ge1-O1-Ge2-O1- linkages (Figures 4d, f-k). The distance of between two same type chains running along the *c* axis is the same as the length of the *c* axis (14.614 Å).

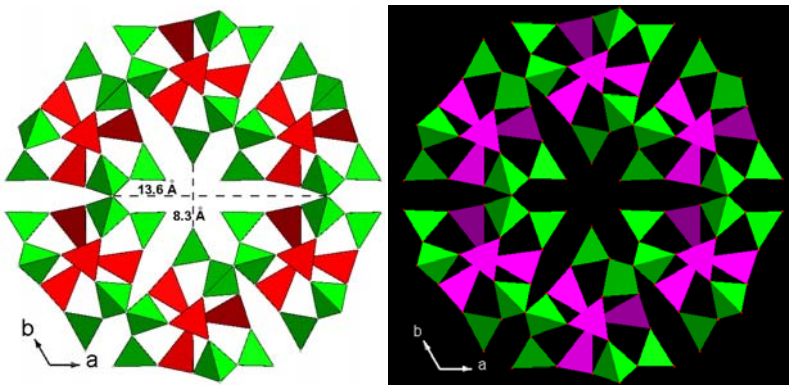

Figure S5. The 24-ring channel with the dimensions of about 8.3 × 13.6 Å in the structure of FJ-1a. The $[Ni2(en)_3]^{2+}$ complex cations filled in the center of the 24-ring channel, achiral trigonal prismatic $[Ni3(en)_3]^{2+}$ complexes occluded between the same chiral structural motifs, and hydrogen atom of OH groups are omitted for clarity. Color code: GeO_4 green, GeO_3Ni red (left); GeO_4 green, GeO_3Ni purple (right).

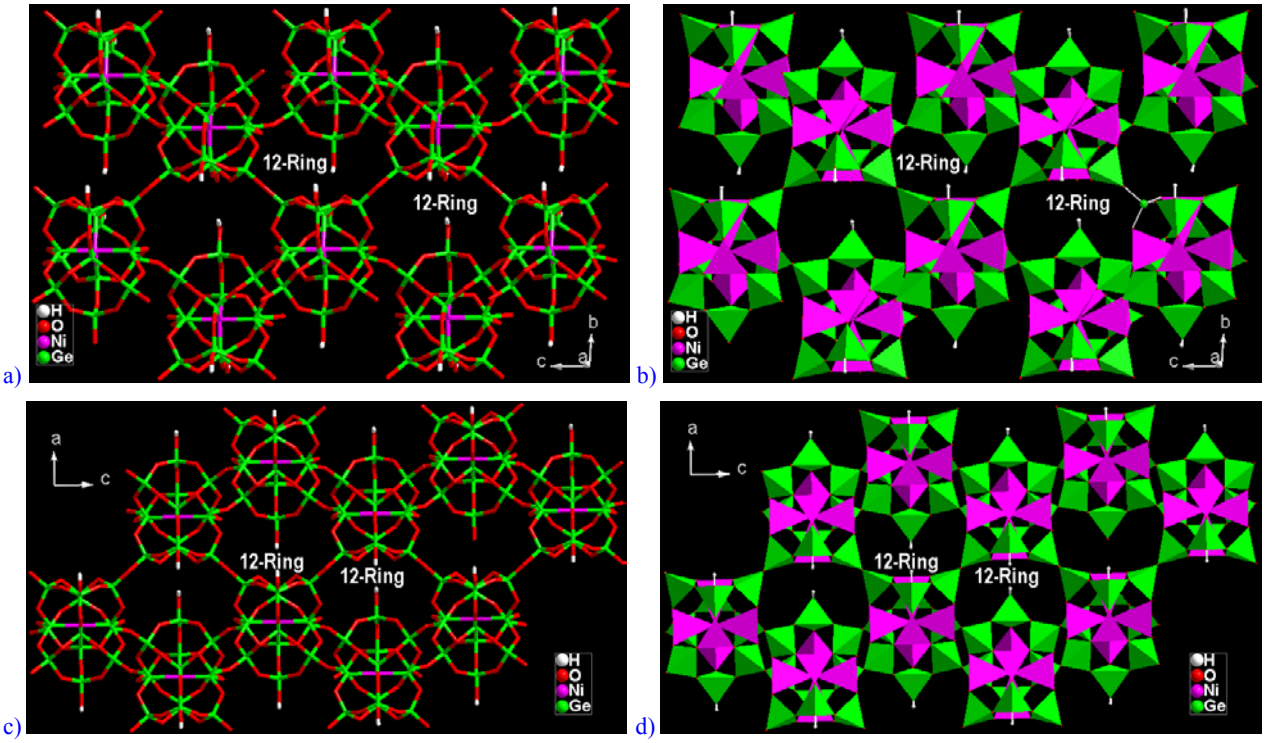

Figure S6. a) and b) Topological and polyhedral view of FJ-1a's framework with 12-ring along the *a* axis, respectively. The achiral $[Ni3(en)_3]^{2+}$ complex cations located in the 12-ring are omitted for clarity. c) and d) Topological and polyhedral view of FJ-1a's framework with 12-ring along the *b* axis, respectively. The achiral $[Ni3(en)_3]^{2+}$ complex cations located in the 12-ring are omitted for clarity.

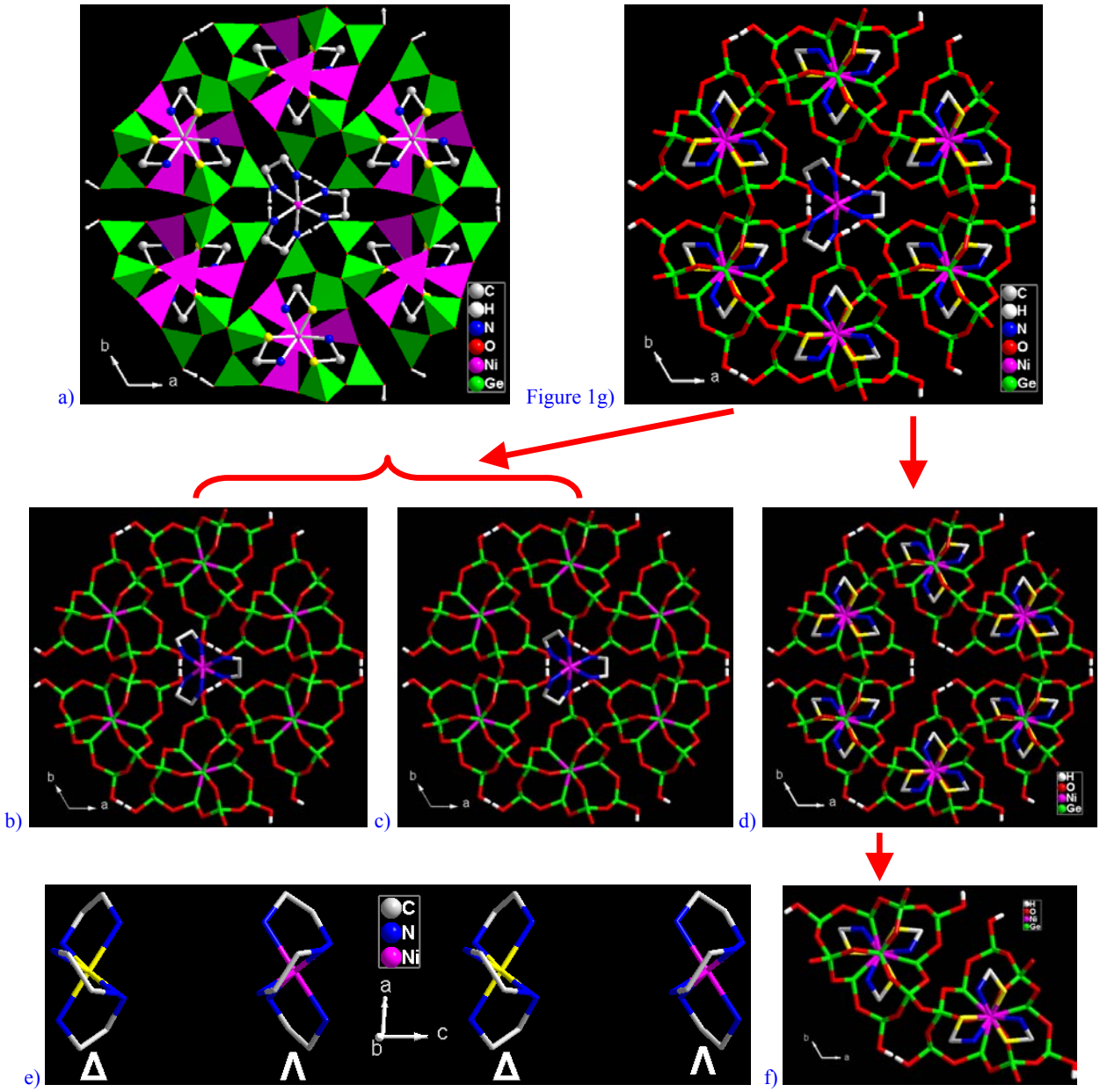

Figure S7. a) and **Figure** 1g) Polyhedral and topological view of the stacking sequence of the 24-ring channel and the relationship between two types of metal complexes (chiral $[Ni2(en)_3]^{2+}$ and achiral $[Ni3(en)_3]^{2+}$ cations) and the inorganic structural motifs, $Ni@Ge_{14}$, in FJ-1a, showing the orderly separation of chiral $[Ni2(en)_3]^{2+}$ complexes filled in the center of the 24-ring channel and achiral trigonal prismatic $[Ni3(en)_3]^{2+}$ complexes occluded between the same chiral structural motifs along the *c* axis. The H atoms of C and N atoms are omitted for clarity. Notably, adjacent inorganic structural motifs of $Ni@Ge_{14}$ in the 24-ring channel of FJ-1a are a pair of enantiomers with Δ- and Λ-$Ni@Ge_{14}$ configurations arranged alternately around the chiral $[Ni2(en)_3]^{2+}$ complexes in the *ab* plane (Figures 1g, S7a-d). A void space analysis with PLATON indicates that the extra-framework species of metal complexes occupies 51.1% of the unit cell volume (A. L. Spek, *Acta Crystallogr. A*, **1990**, *46*, C34). b) and c) The Δ- and Λ-$[Ni2(en)_3]^{2+}$ cations located in the center of the 24-ring channel in the structure of FJ-1a along the *c* axis, respectively. d) The achiral $[Ni3(en)_3]^{2+}$ cations with different orientation in the *ab* plane are separated, respectively, by the $Ni@Ge_{14}$ structural motifs with the same chiral configuration along the *c* axis. Color code: N2, blue; N2', yellow. e) View of chiral enantiomers of $[Ni2(en)_3]^{2+}$ complexes arranged alternately as Δ and Λ configurations in the 24-ring channels along the *c* axis. Color code: yellow Ni2, Δ-configuration; purple Ni2, Λ-configuration. f) View of a pair of enantiomers with Δ and Λ configurations of adjacent $Ni@Ge_{14}$ motifs, also showing adjacent achiral $[Ni3(en)_3]^{2+}$ complexes with two different orientation in the *bc* plane in FJ-1a, showing the symmetry of achiral $[Ni3(en)_3]^{2+}$ complexes with trigonal prism matched that of the inorganic structural motif of $Ni@Ge_{14}$ motif. All hydrogen atoms of C and N atoms are omitted for clarity.

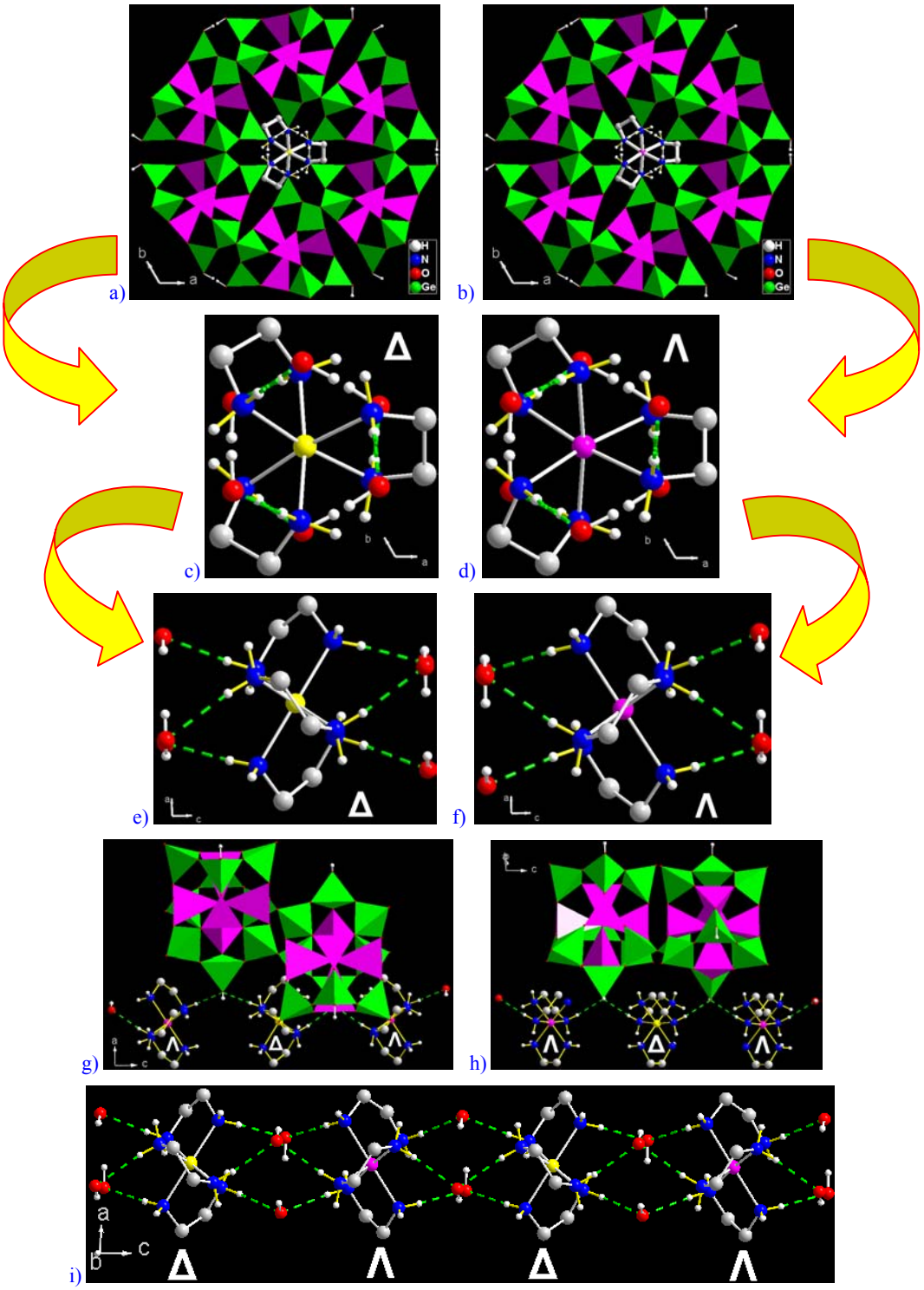

Figure S8. a) and b) Chiral $[Ni2(en)_3]^{2+}$ complexes with Δ and Λ configurations located in the center of the 24-ring channel constructed from six $Ni@Ge_{14}$ structural motifs and interacted with six O(6)H groups from six $Ni@Ge_{14}$ motifs via six hydrogen bonds (H-bonds) in the *ab* plane, respectively. The H atoms of C atoms are omitted for clarity, similarly hereinafter. Color code: yellow Ni2 in $[Ni2(en)_3]^{2+}$ complex, Δ configuration; purple Ni2 in $[Ni2(en)_3]^{2+}$ complex, Λ configurations, $Ge(1,2)O_4$ tetrahedra (green); $Ge(3,4)O_3Ni$ tetrahedra (purple), similarly hereinafter. c) and d) Chiral $[Ni2(en)_3]^{2+}$ complexes with Δ and Λ configurations interacted with six O(6)H groups from six $Ni@Ge_{14}$ motifs via six H-bonds in the *ab* plane, respectively. H-bonds: green line of dashes, similarly hereinafter. The Ni1, Ni3, Ge and O1-O5 atoms are omitted for clarity. e) and f) Chiral $[Ni2(en)_3]^{2+}$ complexes with Δ and Λ configurations interacted with six O(6)H groups from six $Ni@Ge_{14}$ motifs via six H-bonds in the *ac* plane respectively. The H-bond distances N1···O6, 3.072(16) Å. g) and h) Each chiral Δ- and Λ-$[Ni2(en)_3]^{2+}$ complexes interacted with two O(6)H groups from adjacent two $Ni@Ge_{14}$ motifs with Δ- and Λ-

configuration via two H-bonds in the *ac* and *bc* plane, respectively. i) Chiral Δ- and Λ- $[Ni2(en)_3]^{2+}$ complexes interacted with six O(6)H groups from around six Ni@Ge_{14} motifs of three Δ and three Λ configuration, via six H-bonds in the *ac* plane, respectively.

As shown in Figure S8, the chiral $[Ni2(en)_3]^{2+}$ complex cation with regular octahedron has D_3 symmetry; the chiral structural motif of Ni@Ge_{14} cluster has C_3 symmetry that is a subgroup of point-group symmetry of the chiral $[Ni2(en)_3]^{2+}$ complex. As has been previously demonstrated in the work by Morgan, Yu and Xu (see to reference 4 in the text), a chiral microenvironment can be induced by the chiral complex template because of molecular recognition between the host and guest complexes. The analysis of the H-bonds network between chiral $[Ni2(en)_3]^{2+}$ complex template and the structural motifs of Ni@Ge_{14} cluster in FJ-1a can help to understand the chiral molecular recognition and stereo-specificity. Figures 8c-i show the H-bonds arrangement between the chiral $[Ni2(en)_3]^{2+}$ complex and the framework in FJ-1a. Notably, each chiral $[Ni2(en)_3]^{2+}$ complex with Δ configuration forms a total of six H-bonds to six O(6)H groups from adjacent six chiral structural motifs of Ni@Ge_{14} cluster with both the Δ and Λ configuration, or vice versa. The N···O distances are 3.072(16) Å. Furthermore, the H-bonds between the chiral $[Ni2(en)_3]^{2+}$ complex and the chiral structural motifs of Ni@Ge_{14} cluster are related by a threefold symmetry axis. This suggests that the H-bonds imposes the C_3 symmetry operation of a subgroup of point-group symmetry of the chiral $[Ni2(en)_3]^{2+}$ complex (D_3 symmetry) onto the chiral structural motif of Ni@Ge_{14} cluster. It indicates that the chiral molecular recongnition between the chiral guest and chiral motif occurs *via* H-bonds. However, if adjacent Δ- and Λ-configurations of the chiral $[Ni2(en)_3]^{2+}$ complexes along the *c*-axis are exchanged in positions each other, the number of H-bonds will be obviously reduced because of the different orientations of the hydrogen atoms located on the nitrogen atoms. This indicates that H-bonds play a key role in determining the molecular recognition and stereo-specificity between the chiral $[Ni2(en)_3]^{2+}$ complex templates and the inorganic structural motifs of Ni@Ge_{14} cluster. Because Δ, Λ-$[Ni2(en)_3]^{2+}$ configurations are chiral and racemic, it leads to the chirality and racemization of adjacent Ni@Ge_{14} cluster motifs, as well as the achirality of the overall structure of FJ-1 (Figures 1g and S7-8).

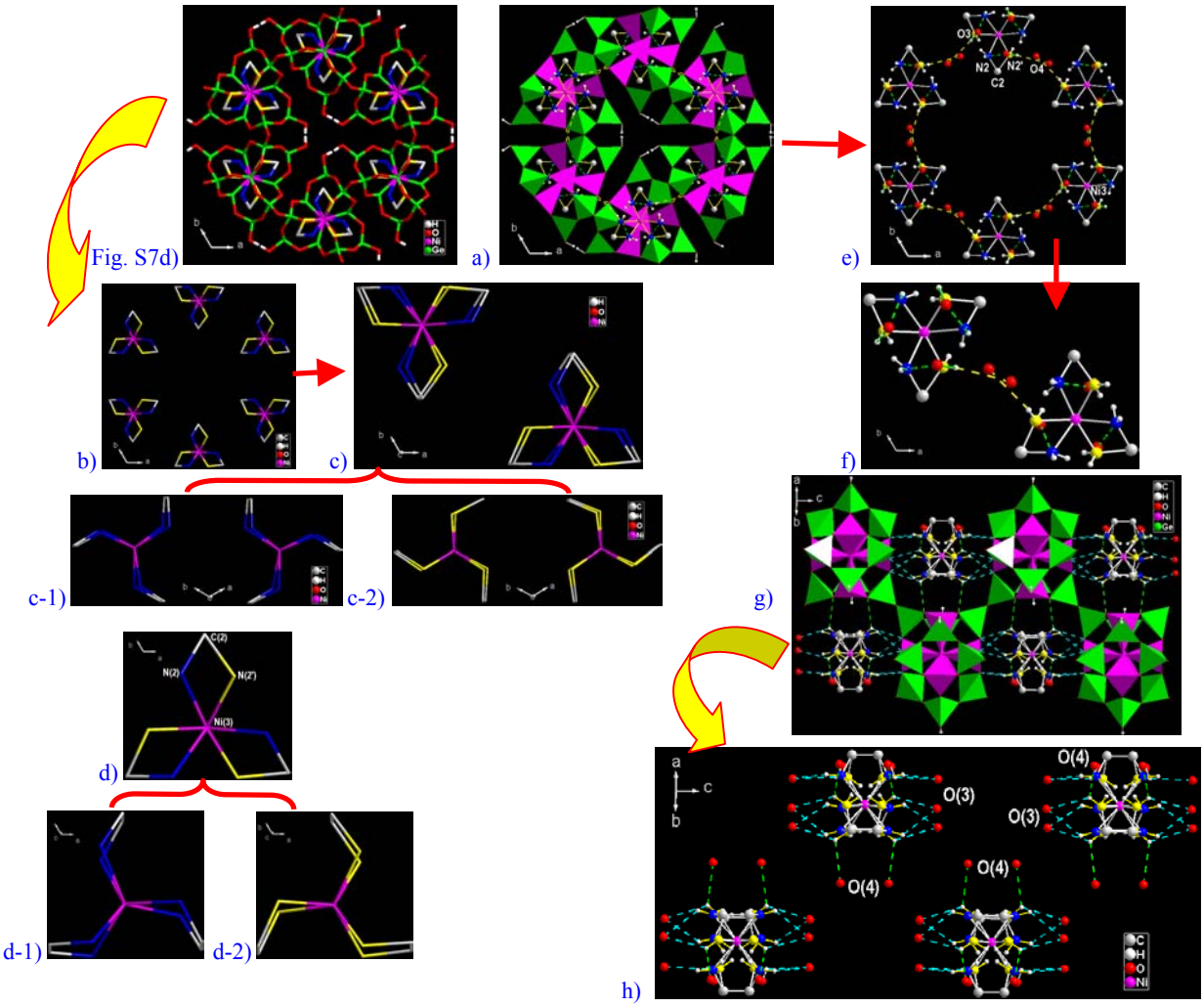

Figure S9. a) Achiral trigonal prismatic $[Ni3(en)_3]^{2+}$ complexes with two different orientations in *ab* plane occluded between the same chiral Ni@Ge_{14} structural motifs along the *c* axis and interacted with O3 and O4 atoms from the Ni@Ge_{14} motifs via H-bonds, respectively. b) Achiral trigonal prismatic $[Ni3(en)_3]^{2+}$ complexes with two different orientations arranged in the *ab* plane. Color code: N2, blue;

N2', yellow, similarly hereinafter. c) Adjacent two achiral enantiomers of $[Ni3(en)_3]^{2+}$ complexes in the *ab* plane. c-1) The two enantiomers of adjacent two $[Ni3(en)_3]^{2+}$ complexes with trigonal prismatic geometries containing N2 atoms in the *ab* plane. c-2) The two enantiomers of adjacent two $[Ni3(en)_3]^{2+}$ complexes with trigonal prismatic geometries containing N2' atoms in the *ab* plane. d) View of the single $[Ni3(en)_3]^{2+}$ complex cation with two sets of trigonal prismatic geometry containing N2 and N2' atoms in FJ-1a along the *ab* plane, showing three mirror symmetry through Ni3 and C2 atoms, respectively, resulting in achiral complex. d-1) and d-2) View of two sets of trigonal prismatic $[Ni3(en)_3]^{2+}$ geometries containing N2 and N2' atoms, respectively. e) View of the H-bonds interactions between the $[Ni3(en)_3]^{2+}$ complexes and the O3 and O4 atoms from $Ni@Ge_{14}$ motifs. f) View of the H-bonds interaction between adjacent two $[Ni3(en)_3]^{2+}$ complexes and adjacent $Ni@Ge_{14}$ motifs. g) View of the H-bonds interactions between $[Ni3(en)_3]^{2+}$ complex and O atoms from $Ni@Ge_{14}$ structural motifs. h) View of the H-bonds interactions between $[Ni3(en)_3]^{2+}$ complex and the O3/O4 atoms from $Ni@Ge_{14}$ structural motifs. The H-bond distances: N2···O3, 3.142(18) Å; N2'···O3, 3.144(9) Å; and N2'···O4, 3.167(20) Å. Color code: the H-bonds for N2'···O4, green lines of dashes; and N2/N2'···O3, cyan lines of dashes. i) View of the symmetry of achiral $[Ni3(en)_3]^{2+}$ complex with trigonal prism matched that of the inorganic structural motif of $[Ni@Ge_{14}O_{24}(OH)_3]^{4-}$ cluster. So did Figure S7f).

i) 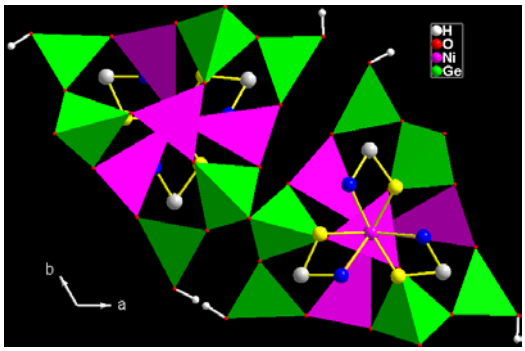

Fig. S7f) 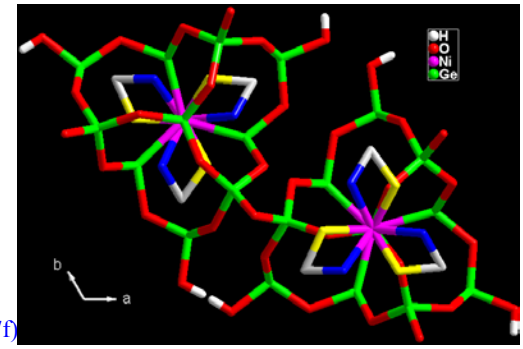

In FJ-1a, the unique N atoms coordinated to Ni3 center occupy two split positions (N2-N2') and have occupancy of 0.5, leading to the formation of rare trigonal prismatic geometry of $[Ni3(en)_3]^{2+}$ complex matched the symmetry of the structural motis. Although adjacent $[Ni3(en)_3]^{2+}$ complexes in the *ab* plane have a mirror image relationship, they are one pair achiral enantiomers because that the N2 and N2' atoms in each $[Ni3(en)_3]^{2+}$ complex possess mirror symmetry each other, leading to achiral $[Ni3(en)_3]^{2+}$ complex; in addition, each $[Ni3(en)_3]^{2+}$ complex cation itself has two sets of trigonal prismatic geometries that contain three mirror symmetry through Ni3 and C2 atoms, resulting in achiral enantiomer (see to Figure S9a-f).

As shown in Figure S9, the $[Ni3(en)_3]^{2+}$ complex cation with two sets of rare trigonal prism consisting of N2 and N2' atoms has D_{3h} symmetry; the chiral structural motif of $Ni@Ge_{14}$ cluster has C_3 symmetry that is also a subgroup of point-group symmetry of the achiral $[Ni3(en)_3]^{2+}$ complex. The analysis of the H-bonds network between achiral $[Ni3(en)_3]^{2+}$ complex and the structural motifs of $Ni@Ge_{14}$ cluster in FJ-1a can help to understand the symmetry transfer from achiral $[Ni3(en)_3]^{2+}$ complex to the structural motif of $Ni@Ge_{14}$ that has not been mentioned in the work by Morgan, Yu and Xu (see to reference 4 in the text). Figures 9e-h show the H-bonds arrangement between the achiral $[Ni3(en)_3]^{2+}$ complex and the framework in FJ-1a. Notably, each achiral $[Ni3(en)_3]^{2+}$ complex forms a total of sixteen H-bonds to six O3 and six O4 from adjacent structural motifs, $Ni@Ge_{14}$ cluster. The N···O distances are 3.142(18)-3.167(20) Å. Furthermore, the H-bonds between the achiral $[Ni3(en)_3]^{2+}$ complex and the structural motifs of $Ni@Ge_{14}$ cluster are related by a threefold symmetry axis. This suggests that the H-bonds also imposes the C_3 symmetry operation of a subgroup of point-group symmetry of the achiral $[Ni3(en)_3]^{2+}$ complex (D_{3h} symmetry) onto the structural motif of $Ni@Ge_{14}$ cluster. It indicates that the symmetry transfers between the achiral guest and the inorganic structural motif occurs *via* H-bonds (Figure S9h, S7d,f). It is worth note that the number of H-bonds will not be changed because of the same orientations of the hydrogen atoms located on the nitrogen atoms, even if the adjacent achiral $[Ni3(en)_3]^{2+}$ complexes along the *c*-axis are exchanged in positions each other. This indicates that there does not exist the molecular recognition and stereo-specificity between the achiral $[Ni3(en)_3]^{2+}$ complexes and the inorganic structural motifs of $Ni@Ge_{14}$ clusters. The H-bonds play only a key role in determining the symmetry transfer between the achiral guest and the inorganic structural motif (Figure S9i, S7d,f).

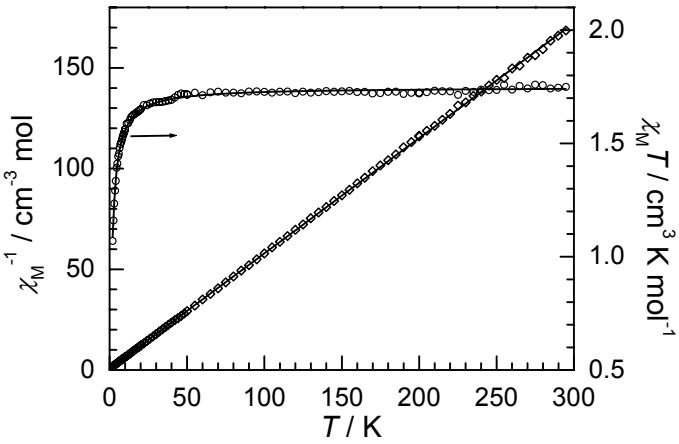

Figure S10. The temperature dependences of the product $\chi_M T$ and χ_M^{-1} for FJ-1a. The Solid lines are the fitting curves of Curie-Weiss law.

In FJ-1a, there exist mixed-valent Ge (Ge^{4+} and Ge^{2+}) and Ni (Ni^{2+} and Ni^{+}) atoms in which the low valent Ge^{2+} and Ni^{+} ions were reduced from the Ge^{4+} and Ni^{2+} ions by amine as reductive reagent under solvothermal conditions. For Ni^{2+} cation, its electron configuration is d^8 (S =1), while for Ni^0, it has d^{10} (S = 0), not d^8s^2 configuration in solid (see to J. M. Goicoechea, S. C. Sevov, *Angew. Chem.* **2005,** *117*, 4094; *Angew. Chem. Int. Ed.* **2005**, *44*, 4026). Thus, the Ni^{+} with d^9 configuration (S =1/2) in FJ-1a is reasonable and confirmed by the variable temperature magnetic susceptibility. Interestingly, there are two types of coordination geometries for $[Ni(en)_3]^{2+}$ complexes in FJ-1a, one is a regular octahedral $[Ni2(en)_3]^{2+}$ cation, another is a rare trigonal prismatic $[Ni3(en)_3]^{2+}$ cation (Figures S8-9). It is notable that the nitrogen coordinated the Ni3 atom occupy two split positions (N2-N2') and have occupancy of 0.5, owing to the requirement of the symmetry of the structural motif, leading to two sets of trigonal prismatic $[Ni3N2_6]$ and $[Ni3N2'_6]$ geometries (Figure S9). Two split N atoms enable $[Ni3(en)_3]^{2+}$ complex to form rare trigonal prismatic $[Ni3N(2,2')_6]$ geometries in high degree of disorder and might lead to the nonmagnetic state of the $Ni3^{2+}$ cation that confirmed by the variable temperature magnetic susceptibility. The details have been discussed in text.

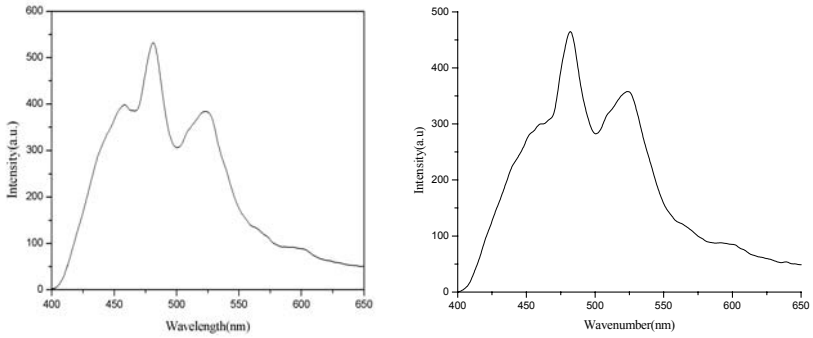

(a) (b)

Figure S11. a) The solid-state fluorescent spectrum of FJ-1a (λ_{ex} = 200 nm) at room temperature. b) The solid-state fluorescent spectrum of FJ-1b (λ_{ex} = 200 nm) at room temperature.

In generally, the luminescence of the reported open-framework phosphates and germanates is attributed to the presence of various kinds of lattice defects[1] which is different from crystalline porous materials incorporated organic dyes or doped with metal activators.[2] For FJ-1a, the blue luminescence in the solid state at the room temperature gives two strong emission bands at 482 and 523 nm and one shoulder at 458 nm (Figure S11a), indicating that the mechanism of the luminescence emission is more complex than that of phosphates and germanates with single emission wavelength.[1] Except lattice defects, low valent Ge^{2+} with s^2 configuration and metal-to-metal charge-transfer of $Ge^{2+}(4s) \rightarrow Ni^{+}(3d)$ in $Ni@Ge_{14}$ cluster should also make contributions to the luminescence emission[3,4] of FJ-1a. In addition, the luminescence emission of FJ-1b in the solid state at the room temperature is the similar to that of FJ-1a (Figure S11b).

[1] P. Feng, *Chem. Commun.* **2001**, 1668; and references therein.
[2] a) P. Behrens, G. D Stucky, In *Comprehensive Supramolecular Chemistry*, ed. G. Albert and T. Bein, Elsevier, New York, **1996**; vol. 7, p 721; b) I. Braum, G. Ihlein, F. Laeri, J. U. Nockel, G. Schulz-Ekloff, F. Schuth, U. Vietze, O. Weiss, D. Wohrle, *Appl. Phys. B: Lasers Opt.*, **2000**, *70*, 335.
[3] A. Ranfagni, M. Mugni, M. Viliani, M. P. Fontana, *Adv. Physics*, **1983**, *32*, 823.
[4] G. Blasse, *Progress Solid and Bonding*, **1999**, *42*, 1.

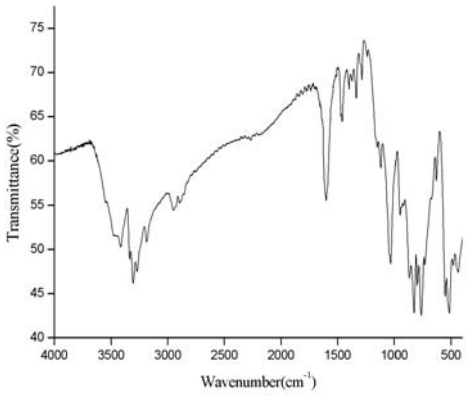

Figure S12. IR spectrum of FJ-1a.

IR spectrum of the FJ-1a shows the stretching bands of the OH, NH_2 and CH_2 groups at ca. 3410, 3180-3330, and 2830-3000 cm^{-1}. The bands at around 1280-1600 cm^{-1} are characteristic of ethylenediamine ligands. The strong band at 1030, 797, 765 cm^{-1} can be assigned to the asymmetric stretching vibrations of Ge-O of GeO_3Ni groups. The peaks at 870 and 827 cm^{-1} correspond to the asymmetric stretching vibrations of Ge-O of GeO_4 tetrahedra. The absorption bands at 550 and 515 cm^{-1} can be assigned to the symmetric stretching vibrations of Ge-O bonds. IR (cm^{-1}): 3415m, 3305s, 3180w, 2950w, 28907w, 1599s, 1457m, 1396w, 1333w, 1284w, 1119w, 1032s, 949 m, 870s, 827s, 763s, 518s.

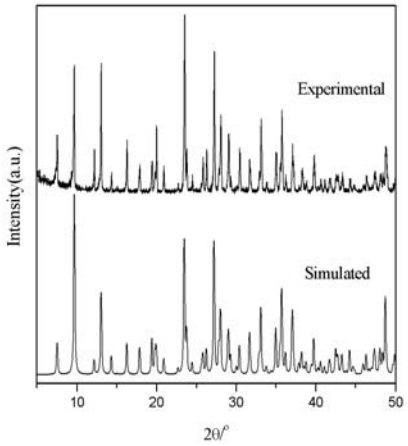

Figure S13. Simulated and experimental powder X-ray diffraction pattern of FJ-1a.

The experimental powder XRD pattern of as-synthesized FJ-1a is in well accord with the one simulated on the basis of the single-crystal structure, indicating phase purity. The difference in reflection intensities between the two patterns was due to the variation in preferred orientation of the power sample during collection of the experimention XRD data.

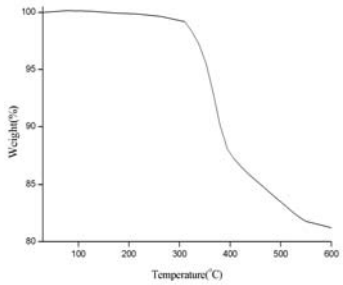

Figure S14. TGA curve of FJ-1a under flowing N_2 atmosphere (10 ºC/min).

TGA carried out in a flow of N_2 atmosphere, showed a weight loss of 18.69% between 300 and 600 ºC. This was attributed to the decomposition of organic molecules in FJ-1a (calcd 18.14%).

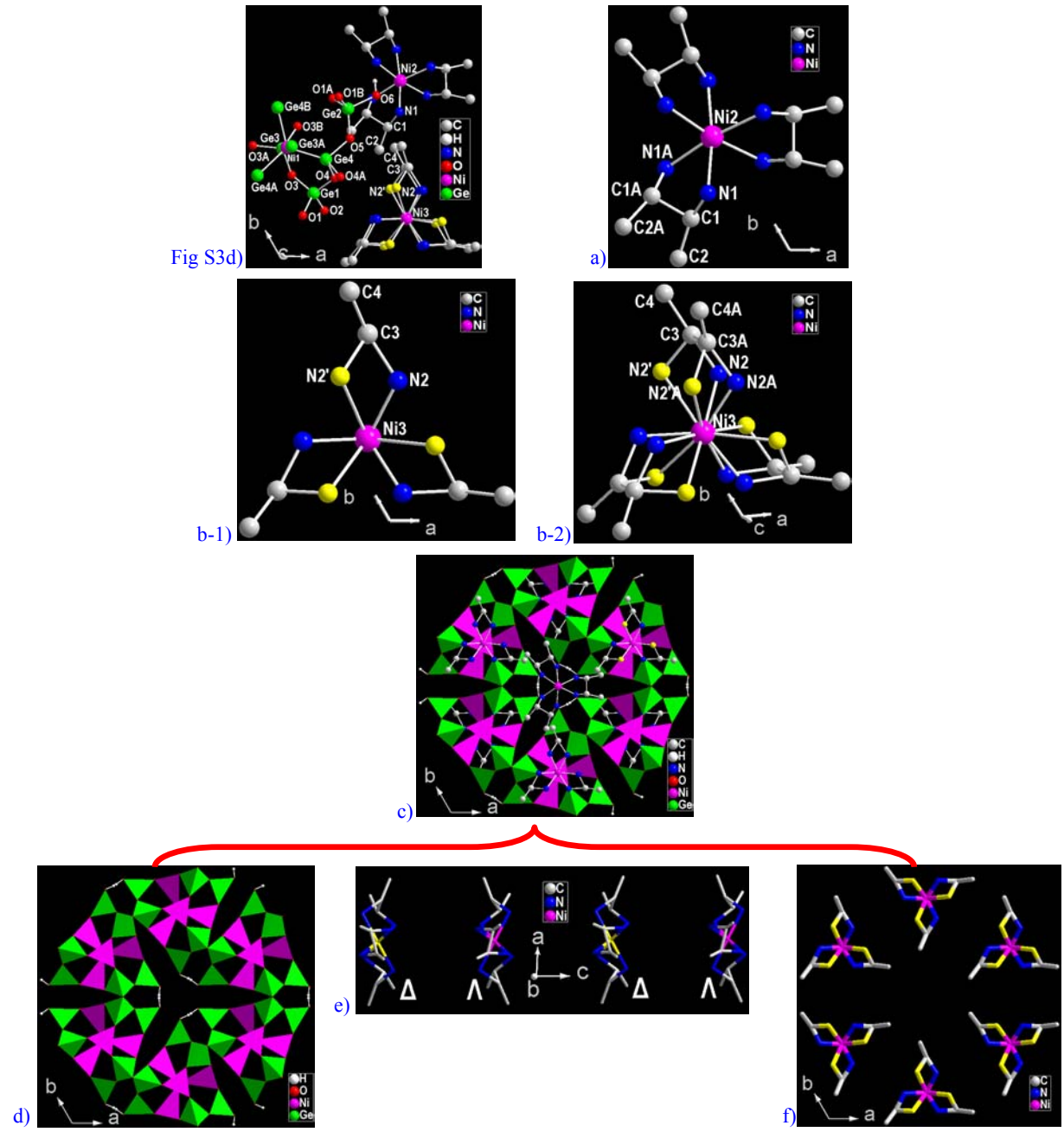

Figure S15. a) View of chiral $[Ni2(enMe)_3]^{2+}$ complex with regular octahedron (D_3 symmetry) in FJ-1b along the *c* axis, showing the C2 (methyl of the enMe) atoms are disorder and have occupancies of 0.5. b-1) and b-2) View of achiral $[Ni3(enMe)_3]^{2+}$ complex with trigonal prism (D_{3h} symmetry) in FJ-1b along the *c* axis and the approximate *c* axis, showing the C4 (methyl of the enMe) atoms are disorder and have occupancies of 0.5 (N2/N2' blue/yellow, similarly hereinafter). c) Polyhedral view of the stacking sequence of the 24-ring channel and the relationship between two types of metal complexes (chiral $[Ni2(enMe)_3]^{2+}$ and achiral $[Ni3(enMe)_3]^{2+}$ cations) and the inorganic structural motifs, $Ni@Ge_{14}$, in FJ-1b, showing the orderly separation of chiral $[Ni2(enMe)_3]^{2+}$ complexes filled in the center of the 24-ring channel and achiral trigonal prismatic $[Ni3(enMe)_3]^{2+}$ complexes occluded between the same chiral structural motifs along the *c* axis. The H atoms of C and N atoms are omitted for clarity. Notably, adjacent inorganic structural motifs of $Ni@Ge_{14}$ in the 24-ring channel of FJ-1b are a pair of enantiomers with Δ- and Λ-$Ni@Ge_{14}$ configurations arranged alternately around the chiral $[Ni2(enMe)_3]^{2+}$ complexes in the *ab* plane. d) View of the framework of FJ-1b that is similar to that of FJ-1a. e) View of chiral enantiomers of $[Ni2(enMe)_3]^{2+}$ complexes arranged alternately as Δ and Λ configurations in the 24-ring channels along the *c* axis. Color code: yellow Ni2, Δ-configuration; purple Ni2, Λ-configuration. f) Achiral trigonal prismatic $[Ni3(enMe)_3]^{2+}$ complexes with two different orientations arranged in the *ab* plane.